ENVIRONMENTAL ENGINEERING SCIENCE
Volume 26, Number 1, 2009

DOI: 10.1089/ees.2007.0180

Application of Computational Fluid Dynamics for Optimal Design of Horizontal-Flow Baffled-Channel Powdered Activated Carbon Contactors

Young-Il Kim,[1] Chang-Jin Ahn,[2] Chae-Young Lee,[3] and Byung-Uk Bae[4,*]

[1]*Chungcheongnamdo Watershed Management Research Center,Chungnam Development Institute, 112-1 Yongdu-dong, Jung-gu, Daejeon, 301-745, Republic of Korea.*
[2]*Department of Water Supply Operation & Management, Korea Water Resources Corporation, San 6-2 Yeonchuk-dong, Daedeok-gu, Daejeon, 306-711, Republic of Korea.*
[3]*Department of Civil Engineering, The University of Suwon, San 2-2, Wau-ri, Bongdam-eup, Hwasung, Gyunggi Province, 445-743, Republic of Korea.*
[4]*Department of Environmental Engineering, Daejeon University, 96-3 Yongun-dong, Dong-gu, Daejeon, 300-716, Republic of Korea.*

Received: July 18, 2007 *Accepted in revised form: March 20, 2008*

Abstract

For more efficient design of a horizontal-flow baffled-channel powdered activated carbon (PAC) contactor (hBPC), which might be used to cope with taste and odor problems at conventional water treatment plants, computational fluid dynamics (CFD) using FLOW-3D was applied. In order to verify the performance of the CFD simulations, the experimental results of tracer tests from a pilot-scale hBPC were compared to those from the simulation. Results from the CFD simulation were very similar to those of the tracer tests. Velocity distributions showed that there were stagnant regions on the back side of the baffles. These stagnant regions would be expected to decrease the overall adsorption efficiency of the PAC particles. The size of the stagnant regions and retention times in the simulated hBPC increased as the length to width (L/W) ratio increased and the bend width decreased. The L/W ratio, bend width, and the number of baffles for optimal design of the hBPC were successfully generated by the simulation. When designing a full-scale hBPC, the designer should consider the L/W ratio, number of baffles, and bend width in order to maximize the hBPC performance.

Key words: computational fluid dynamics (CFD); powdered activated carbon (PAC); horizontal-flow baffled-channel PAC contactor (hBPC); bend width; length to width ratio (L/W)

Introduction

POWDERED ACTIVATED CARBON (PAC) has been widely used for coping with taste and odor (T&O) episodes in drinking water supplies (Suffet *et al.*, 1995). The efficiency of PAC for removing T&O is highly dependent on the contact time, PAC dose, degrees of mixing, and the presence of competing compounds (Lalezary *et al.*, 1988). In conventional water treatment plants (WTP), PAC is commonly added into the rapid mixing basin where other water treatment chemicals, such as coagulants, alkaline chemicals, and chlorine, are added simultaneously. However, when the PAC is added into the rapid mixing basin with other chemicals, the adsorption efficiency of PAC might be adversely affected by those chemicals (Najm *et al.*, 1991).

**Corresponding author:* Department of Environmental Engineering, Daejeon University, 96-3 Yongun-dong, Dong-gu, Daejeon, 300-716, Republic of Korea. *Phone:* +82 422802535; *Fax:* +82 422840109; *E-mail:* baebu@dju.ac.kr

To maximize adsorption efficiency of PAC for T&O removal by minimization of interference with chemicals, a separate horizontal-flow baffled-channel PAC contactor (hBPC) based on the concept of a hydraulic flocculator was proposed for inclusion in a newly constructed WTP in Korea (Ahn, 2003). The baffled-channel contactor (BPC), which would use only hydraulic energy for mixing raw water and PAC, was to be located immediately before the rapid mixing basin. The advantages of a BPC include good performance, if the flow rate is reasonably constant, minimal maintenance due to lack of mechanical equipment, and minimal short-circuiting (Schulz and Okun, 1984).

In a recent paper, results were published in which the hydrodynamic characteristics of a pilot-scale hBPC were investigated by tracer tests under different operating conditions, such as the number of baffles and dimensions of the flow paths (Kim and Bae, 2007). In the present study, computational fluid dynamics (CFD) simulations using the commercial software FLOW-3D was applied for more exact and efficient design of the full-scale hBPC (Sicilian *et al.*, 1987).

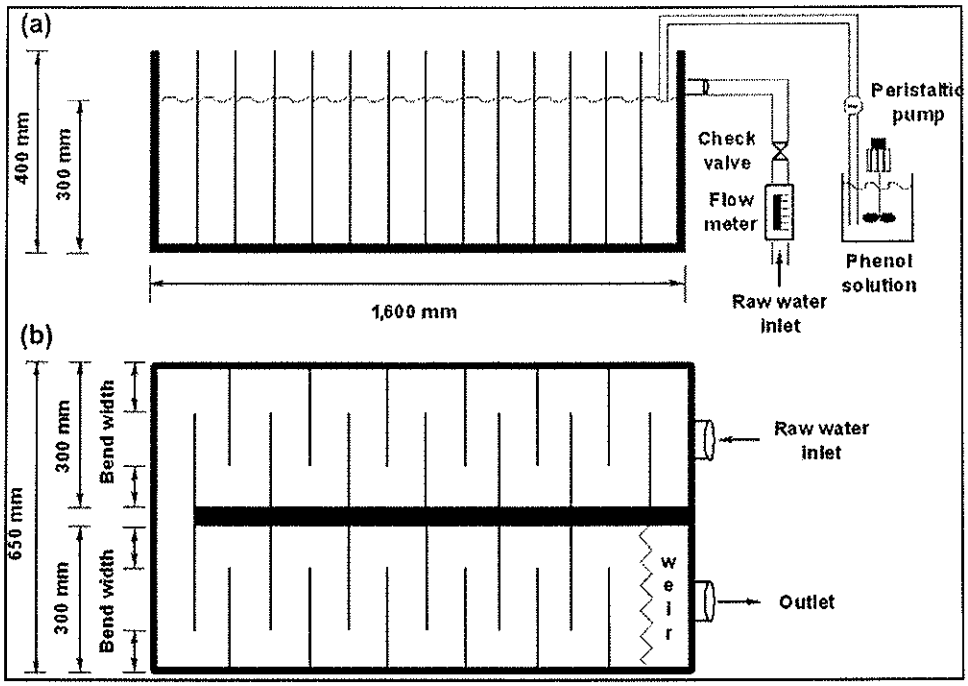

FIG. 1. Schematic diagram of pilot-scale hBPC: (a) cross-sectional view, (b) plan view.

In this research, CFD simulation results were first compared with the results of experimental tracer tests (Templeton *et al.*, 2006). After ascertaining that CFD could be a valuable tool for the efficient design of hBPCs, the effects of contactor configuration and interior details on the hydrodynamic behavior of the hBPC were investigated.

Materials and Methods

Experimental tracer tests using a pilot-scale hBPC

Figure 1 shows the pilot-scale hBPC with a working volume of 288 liters used for tracer tests. The length of the pilot-scale hBPC was 1,600 mm; the width and height were

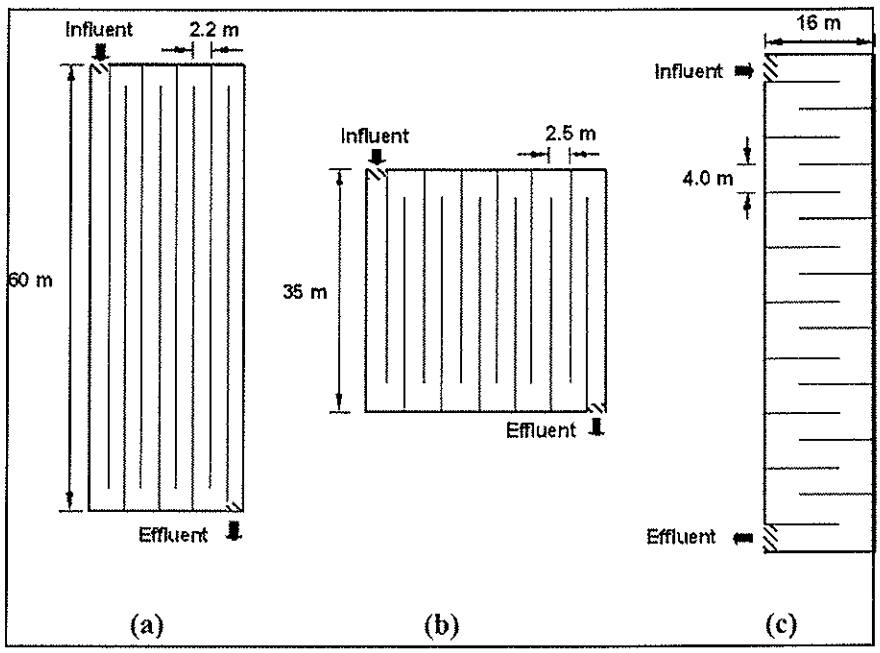

FIG. 2. Configuration of simulated full-scale hBPCs according to variations of L/W ratio: (a) L/W = 28:1, (b) L/W = 14:1, (c) L/W = 4:1.

650 mm and 400 mm, respectively. The channel of 1,600 mm length by 300 mm of width and effective water depth matched. To install various sized baffles, 25 grooves were made on the inside walls of the contactor. The effluent was withdrawn over a weir located at the end of the contactor. The step input tracer tests were conducted for the pilot-scale hBPC at 20 minutes of contact time using 4 mg/L of phenol as in a recent published paper (Kim and Bae, 2007). Bend widths (the distance between the end of baffle and the side wall of contactor; refer to Fig. 1) of 30 and 90 mm for the pilot-scale hBPC were tested with sets of 13 and 25 baffles, respectively. Samples of effluent were taken every two minutes and analyzed for the concentration of phenol. Generally, step inputs were done to analyze the retention time distribution of effluent water in the PAC contactor (Teefy, 1996). The complete mixing and plug flow fractions were estimated using both index analysis and graphic analysis (Hart and Gupta, 1978; Hudson, 1981; Rebhun and Argaman, 1965). Phenol was measured in accordance with the proposed Method 5530D in Standard Methods (APHA, 1998).

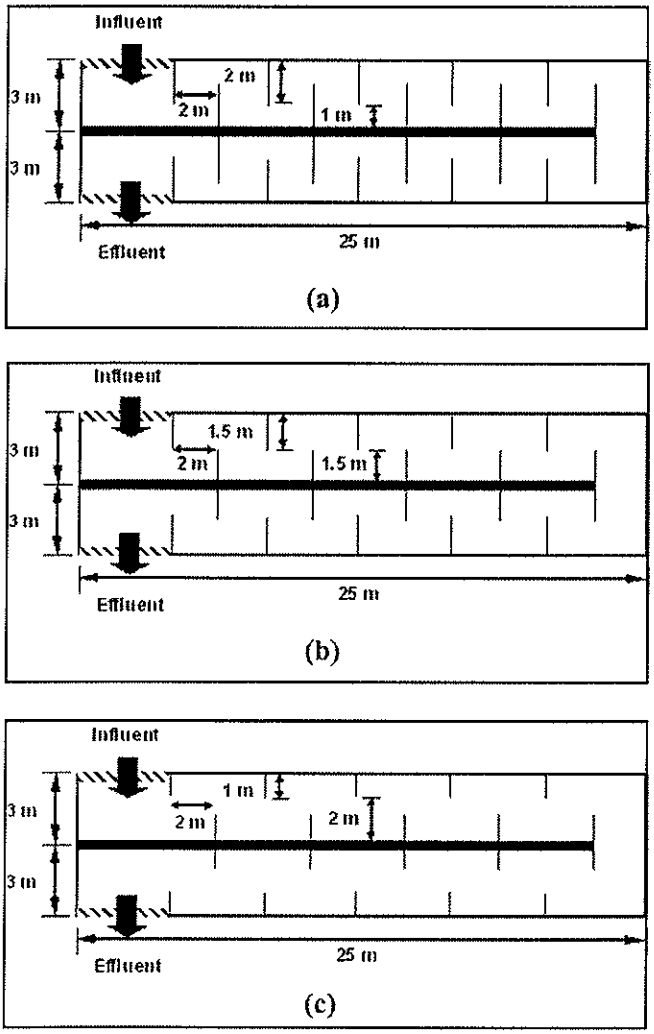

FIG. 3. Configuration of simulated full-scale hBPCs according to variations of bend width and baffle: (a) bend width at 30% of total width, (b) bend width at 50% of total width, (c) bend width at 70% of total width.

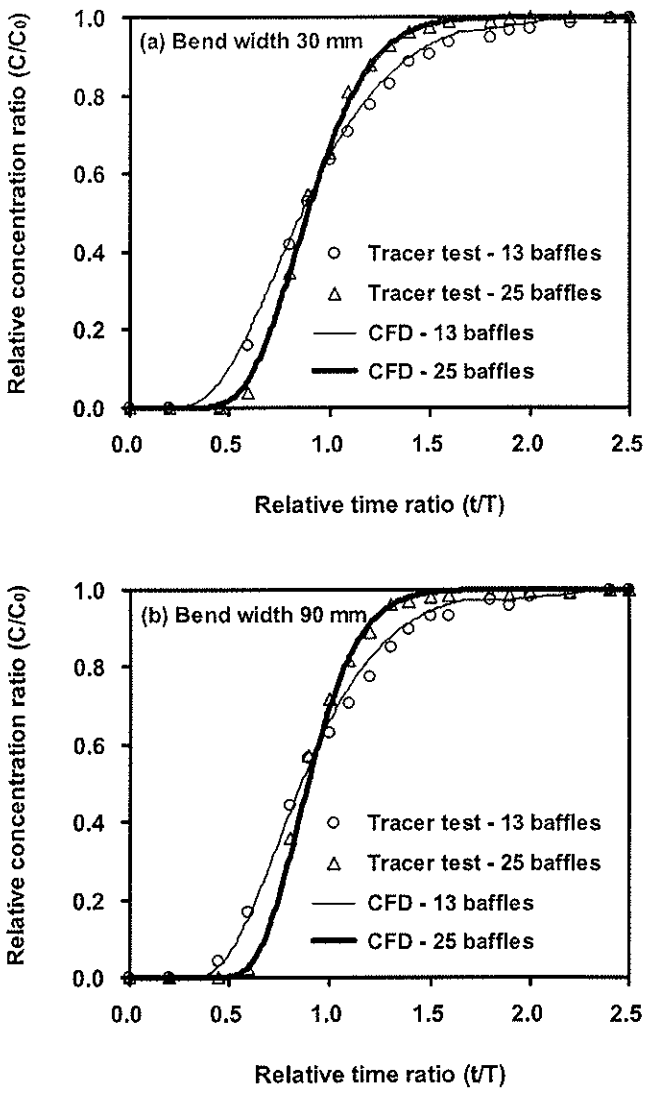

FIG. 4. Tracer curves and CFD simulations of various bend widths and numbers of baffles in a pilot-scale hBPC. Baffle dimension: (a) 270 W × 350 mm H, (b) 210 W × 350 mm H.

Verification of CFD simulations based on tracer tests using a pilot-scale hBPC

The CFD simulation was performed using FLOW-3D (ver. 7.7, Flow Science Inc.), which is commercially available. In order to verify the CFD simulations, the CFD simulated tracer tests were compared with tracer tests conducted with a pilot-scale hBPC under the same conditions. The pilot-scale hBPC geometries were created using 3-dimensional computer aided design (CAD) and then transferred to FLOW-3D. The pilot-scale hBPC geometries were defined using 3-dimensional FAVOR (fractional area and volume ratios) and the computational grid was 73 cells long, 26 cells wide, and 27 cells high. The FAVOR allows the geometry to be defined exactly, with the mesh of computational cells being mapped onto the boundaries of the geometry. The time-averaged Navier-Stokes equations for momentum and continuity were solved for steady, incompressible, turbulent, and isothermal flow. The standard κ–ε turbulence model was used for mod-

TABLE 1. INDICES FROM EXPERIMENTAL TRACER TESTS WITH VARIATIONS OF NUMBERS OF BAFFLE AND BEND WIDTHS

Bend width / *Number of baffles*	t_{90}/t_{10}	t_a/T	t_i/T	t_{10}/T	p (%)	$1-p$ (%)	m (%)
30 mm—25	1.80	1.00	0.50	0.75	83	17	−5
30 mm—13	2.67	1.00	0.50	0.66	64	36	−8
90 mm—25	1.73	0.99	0.50	0.72	77	23	3
90 mm—13	2.50	0.95	0.30	0.56	65	35	−6

Note: T = theoretical retention time; t_{90} = time when 90% of tracer is recovered, t_{10} = time when 10% of tracer is recovered, t_a = averaging retention time, t_i = time when tracer is initially detected, t_{90}/t_{10} = Morrill dispersion index, t_a/T = index of dead space, t_i/T = index of short circuiting, $t_{10}/T = t_{10}$ as percentage of T, p (%) = fraction of active flow volume acting as plug flow, 1 − p (%) = fraction of active flow volume acting as mixed flow, m (%) = fraction of dead space volume in the total volume.

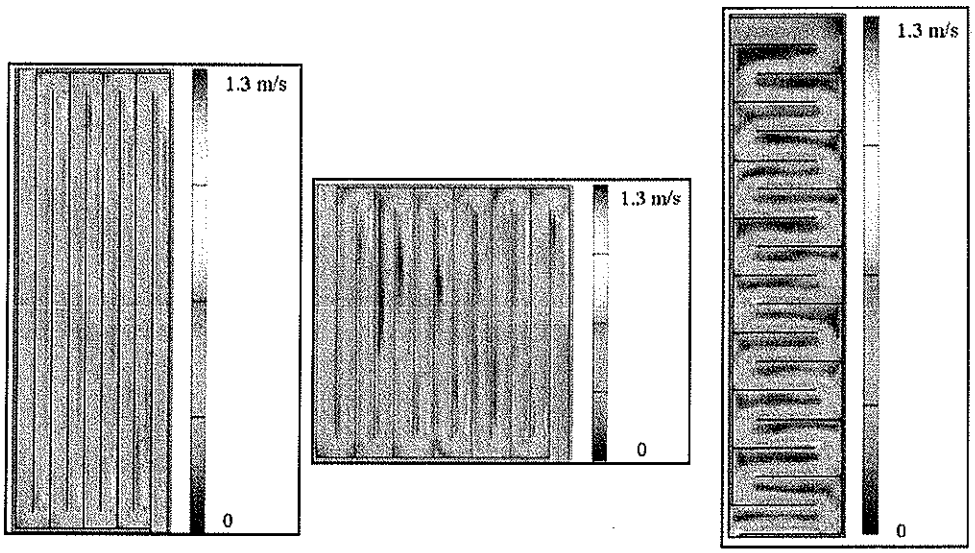

FIG. 5. Simulation of velocity distribution in full-scale hBPCs with variations of L/W ratio. (a) L/W = 28:1, (b) L/W = 14:1, (c) L/W = 4:1.

eling the turbulence transport of momentum (Versteeg and Malalasekera, 1995). For setting up the boundary condition at inlet and outlet, the longitudinal velocity component was set to the value of the mean inlet velocity calculated using volumetric flow rate and area. The position of the free surface at the outlet was set at 0.3 m, the same depth measured during the experimental tracer tests.

Application of CFD simulations to variations of hBPC configuration for efficient design of full-scale hBPCs

After ascertaining that CFD could simulate the tracer tests using a pilot-scale hBPC, two simulations were run based on the specific full-scale hBPCs. The design capacity of full-scale hBPCs for first simulations was 36.750×10^4 m^3/d with 20 minutes of theoretical retention time. The three length/width (L/W) ratios were used: 28:1 (length: 60.0 m, width: 2.2 m, 8 baffles), 14:1 (length: 35.0m , width: 2.5 m, 12 baffles), and 4:1 (length: 16.0 m, width: 4.0 m, 17 baffles) (refer to Fig. 2). Virtual PAC particles were used in the simulation. The number of virtual PAC particles in the effluent was measured af-

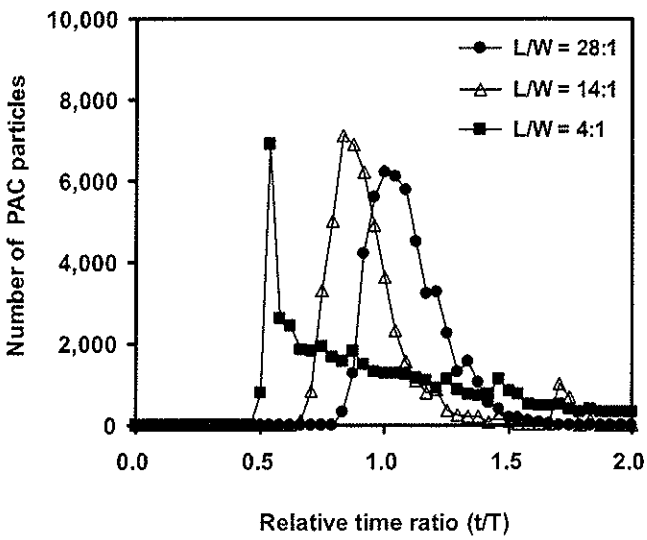

FIG. 6. Tracer curves of number of particles with variations of L/W ratio.

ter adding 50,000 virtual PAC particles to the influent. After finishing the simulation, the velocity in the hBPC was calculated and PAC particle breakthrough curves were made to calculate the mean retention time (Teefy and Singer, 1990). The PAC particles were assumed to be spherical and approximately the same density as the PAC. The average diameter and density of the PAC particles were 0.025 mm and 1.125 g/cm^3, respectively. The boundary conditions at inlet and outlet for solving the simulations were velocity and depth, respectively.

Figure 3 shows the configuration of the full-scale hBPC for the second simulations. The design capacity of the full-scale hBPC was 3.255×10^4 m^3/d with 20 minutes of theoretical retention time. When the water depth was 3 m, the length and width of the channel in the full-scale hBPC were 25 and 3 m, respectively. For the simulation, the bend width was set at either 30, 50, or 70% of total width in the same full-scale hBPCs. Ten thousand virtual PAC particles were added to the influent to calculate the velocity and mean retention time of the hBPC. The other parameters were the same as in the previous simulation.

Results and Discussions

Verification of CFD simulations based on tracer tests using a pilot-scale hBPC

Figure 4 compares the results of the experimental tracer test and CFD simulations at the 90 mm (30% of total width) and 30 mm (10% of total width) bend widths according to the number of baffles in the hBPC. The results of the CFD simulation were very similar to those from experimental tracer tests conducted with the hBPC. Table 1 shows the indices calculated from analysis of the experimental tracer test results. The percent of plug flow and t_{10}/T values increased when the bend width decreased. The PAC adsorption efficiency increased as the percent of plug flow increased because the retention time of the PAC particles reached the theoretical retention time.

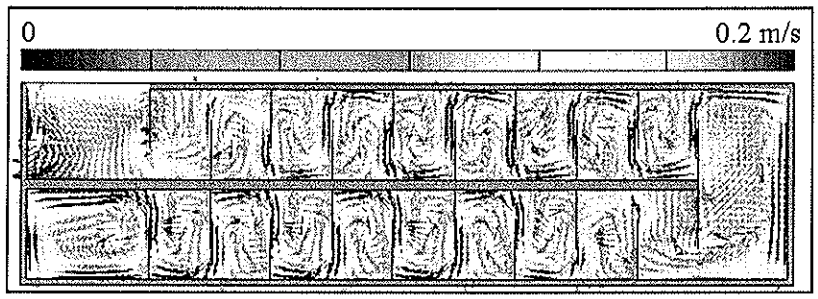

(a)

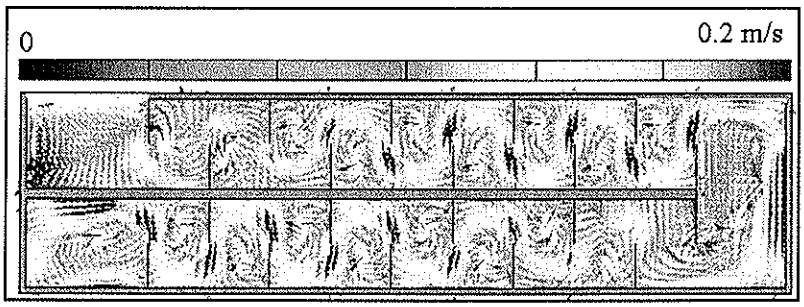

(b)

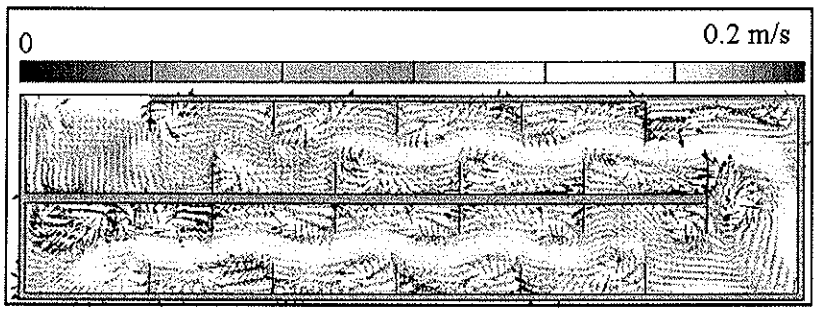

(c)

FIG. 7. Simulation results of velocity distribution in full-scale hBPCs with variations of bend width: (a) bend width at 30% of total width, (b) bend width at 50% of total width, (c) bend width at 70% of total width.

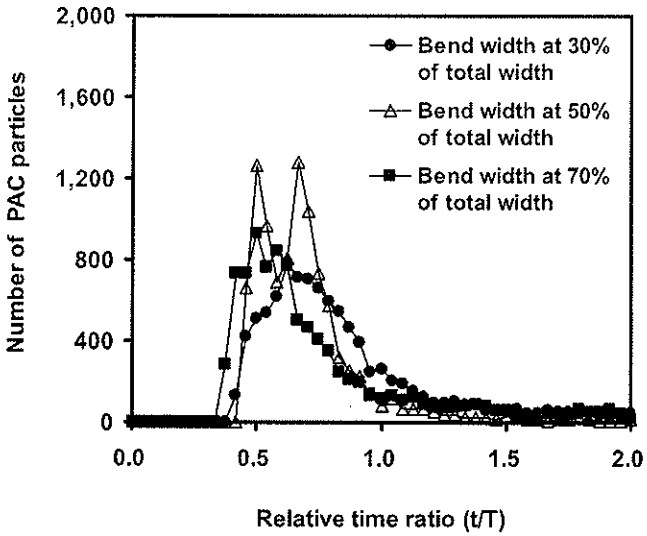

FIG. 8. Tracer curves of number of particles with variations of bend width.

Application of CFD simulations to variations of hBPC configuration for efficient design of full-scale hBPCs

Figure 5 shows the simulation results of velocity distribution with various L/W ratios. The velocity distribution showed that there were some stagnant regions on the back sides of the baffles. The stagnant portion increased as the L/W ratio decreased. Figure 6 shows the tracer curves of the number of PAC particles used to compute the actual retention time with variations of the L/W ratio. For L/W ratios of 14:1 and 4:1, the PAC particles exited the contactor faster than the theoretical retention time of 20 minutes. On the other hand, at the L/W ratio of 28:1, the contactor mean retention time equaled the theoretical retention time. The peak of the PAC particle breakthrough curve at the L/W ratio of 4:1 was two times faster than that at 28:1. Figure 7 shows the simulation results of velocity distribution with three different dimensions of bend width. In the case of Fig. 7(a), the average velocity calculated from simulations between baffles in the channels was 0.063 m/sec, when the velocity in the bends was 0.135 m/sec. As suggested visually, the velocity on the back side of the baffles was much slower than the average velocity, while that on the front side of the baffles and in the bends were faster than the average velocity (Hannoun *et al.*, 1998). Stagnant regions of slow velocity also showed up on the back sides of baffles as in previous simulations. These stagnant regions would be expected to decrease the adsorption efficiency of PAC particles. As shown in Fig. 8, the PAC particle breakthrough curve did not vary significantly with bend width variation. The majority of the PAC particles exited the contactor two times faster than the theoretical retention time of 20 minutes. When the bend width was set at 30% of total width, the mean retention time was 16 minutes based upon the analysis of PAC particle breakthrough curve. However, when the bend width was set at either 50 or 70% of total width, the mean retention time was around 14 minutes. The mean retention time in the hBPC was not much affected by variations of bend width even though the velocity was affected.

Table 2 shows summaries of CFD simulations with variations of L/W ratio and bend width. The plug flow portion increased as L/W ratio increased (Bishop *et al.*, 1993). The differences in the plug flow portion among the bend widths tested were not much different than those due to variations in the L/W ratio.

Conclusions

A CFD simulation was applied to increase the design efficiency of hBPCs widely used in Korean WTPs for treating T&O problems. Results from the CFD simulations were very similar to results from experimental tracer tests conducted with the pilot-scale hBPC. Simulation results on the distribution of PAC particles showed that there were some stagnant regions on the back sides of the baffles in which PAC particles would not be mixed. The stagnant regions and retention time in the hBPC increased as the length to width (L/W) ratio increased; when bend width decreased. The

TABLE 2. SUMMARIES OF CFD STIMULATION WITH VARIATIONS OF L/W RATIO AND BEND WIDTH

Conditions		t_{90}/t_{10}	t_a/T	t_i/T	t_{10}/T	p (%)	$1-p$ (%)	m (%)
L/W ratio	28:1	1.40	1.11	0.83	0.92	88	12	−6
	14:1	1.52	0.98	0.67	0.76	84	16	3
	4:1	2.95	0.99	0.50	0.53	53	47	14
Bend width	30% of total width	2.60	0.85	0.42	0.50	64	36	22
	50% of total width	1.96	0.72	0.46	0.48	76	24	34
	70% of total width	3.10	0.76	0.38	0.42	53	47	33

Note: T = theoretical retention time; t_{90} = time when 90% of particles are recovered, t_{10} = time when 10% of particles are recovered, t_a = average retention time, t_i = time when particles are initially detected, t_{90}/t_{10} = Morrill dispersion index, t_a/T = index of dead space, t_i/T = index of short circuiting, t_{10}/T = t_{10} as percentage of T, p (%) = fraction of active flow volume acting as plug flow, 1 − p (%) = fraction of active flow volume acting as mixed flow, m (%) = fraction of dead space volume in the total volume.

L/W ratio, bend width and the number of baffles for optimal design of the hBPC were successfully generated by the simulation. When designing a full-scale hBPC, the designer should consider the L/W ratio, number of baffles, and bend width in order to maximize the hBPC performance.

Author Disclosure Statement

No competing financial interests exist.

References

Ahn, C.J. (2003). *Improvement of effective taste and odor removal process due to baffled PAC contactor*. Ph.D. Dissertation, Chungbuk National University, Republic of Korea.

APHA, AWWA, WEF. (1998). *Standard Methods for the Examination of Water and Wastewater*,20th ed. Washington, D.C.: American Public Health Association.

Bishop, M.M., Morgan, M., Cornwell, B., and Jamison, D.K. (1993). Improving the disinfection detention time of a water plant clearwell. *AWWA* 85, 68.

Hannoun, I.A., Boulos, P.F., and John List, E. (1998). Using hydraulic modeling to optimize contact time. *AWWA* 90, 77.

Hart, F.L., and Gupta, S.K. (1978). Hydraulic analysis of model treatment units. *J. Environ. Eng. Div., ASCE* 104, 785.

Hudson, H.E. (1981). *Water Clarification Process, Practical Design, and Evaluation*. New York: Van Nostrand Reinhold.

Kim, Y.I., and Bae, B.U. (2007). Design and evaluation of hydraulic baffled-channel PAC contactor for taste and odor removal from drinking water supplies. *Water Res.* 41, 2256.

Lalezary, S., Pirbazari, M., Dale, M.S., Tanaka, T.S., and McGuire, M.J. (1988). Optimizing the removal of geosmin and 2-methylisoborneol by powdered activated carbon. *AWWA* 80, 73.

Najm, I.N., Snoeyink, V.L., Lykins Jr., B.W., and Adams, J.Q. (1991). Using powdered activated carbon: A critical review. *AWWA* 83, 65.

Rebhun, M., and Argaman, Y. (1965). Evaluation of hydraulic efficiency of sedimentation basins. *San. Eng., ASCE* 91, 37.

Schulz, C.R., and Okun, D.A. (1984). *Surface Water Treatment for Communities in Developing Countries*. New York: John Wiley & Sons.

Sicilian, J.M., Hirt, C.W., and Harper, R.P. (1987). *FLOW-3D: Computational modeling power for scientists and engineers*. Flow Science Report (FSI-87-00-1). Santa Fe, NM: Flow Science Inc.

Suffet, I.H., Mallevialle, J., and Kawczynski, E. (1995). *Advances in taste and odor treatment and control*. Denver, CO: AWWARF.

Teefy, S.M. (1996). *Tracer Studies in Water Treatment Facilities: A Protocol and Case Studies*. Denver, CO: AWWARF.

Teefy, S.M., and Singer, P.C. (1990) Performance and analysis of tracer tests to determine compliance of a disinfection scheme with the SWTR. *AWWA* 82, 88.

Templeton, M.R., Hofmann, R., and Andrews, R.C. (2006). Case study comparisons of computational fluid dynamics modeling versus tracer testing for determining clearwell residence times in drinking water treatment. *J. Environ. Eng. Sci.* 5, 529.

Versteeg, H.K., and Malalasekera, W. (1995). *An Introduction to Computational Fluid Dynamics*. Englewood Cliffs, NJ: Prentice Hall.